

Predicting Lock-in on Drilling Risers in Sheared Flows

J. Kim Vandiver

Massachusetts Institute of Technology, Cambridge, Massachusetts, 02139 USA

This paper is from the Proceedings of the Flow-Induced Vibration 2000 Conference, Lucerne, Switzerland, June 18-22, 2000

Corrections to equations 20 and 21 made July 26, 2000.

ABSTRACT: The kurtosis statistic is introduced as a sensitive tool for efficient preliminary analysis of flow-induced vibration response data. The kurtosis of sequential blocks of time series data allows one to distinguish single mode lock-in events. The problem of predicting lock-in is then discussed. Instructional examples are introduced to illustrate the relative importance of flow-speed, power-in length and diameter, when attempting to predict single frequency dominance. When VIV from two different flow speed regions compete, it is shown that the ratio of the flow speeds cubed is an important indicator, as is the ratio of the square of the length of the power-in regions. Two example cases from measured response on a drilling riser in the North Sea are presented. SHEAR7 predictions are compared to measured results.

1 INTRODUCTION

In the past two years BP/Amoco and the Norwegian Deepwater Project have made available vortex-induced vibration (VIV) data from four drilling risers in the North Sea. Although the velocity profiles have shown great variation in speed and direction with depth, single mode dominated response has been frequently observed. The observed single-mode response occasionally has lock-in properties similar to those seen under uniform flow conditions. In particular the onset of lock-in is accompanied by an increase in response amplitude, a dominance of a single frequency and development of constant response amplitude sinusoidal behavior. Finding and classifying these single frequency events can be a tedious exercise, requiring sorting through thousands of multi-channel records of response data. In this paper it is shown that the statistic known as kurtosis is especially useful in detecting lock-in events. By using this statistic it is possible to efficiently sort VIV response according to behavior.

Once lock-in and non-lock-in events are identified, the next step is to understand and explain the flow conditions and the structural dynamic properties that govern the occurrence of lock-in. The final step is to develop response prediction models that are able to predict response behavior.

This paper first presents the use of the statistic kurtosis in the identification of lock-in events. Sec-

ond, simplified instructional examples are used to reveal the relative importance of parameters, such as damping and length of the lock-in region. Third, the MIT VIV response prediction program SHEAR7 is used to predict vibration of a North Sea drilling riser, using measured current profiles. Comparisons are made between measured and predicted VIV.

The author thanks BP-Amoco for the Schiehallion riser data, and the Norwegian Deepwater Programme (BP-Amoco, Esso, Norsk Hydro, Saga, Shell, Statoil, Conoco, Mobil) for the Helland Hansen Riser Data."

2 USING KURTOSIS FOR LOCK-IN IDENTIFICATION

Typical drilling riser response measurements are from instruments strapped to the riser at several different positions. Assume that $x(t)$ is a zero mean, measured time series of transverse acceleration response, resulting from VIV. The kurtosis of $x(t)$ is given by:

$$\text{kurtosis} = \frac{\langle x^4 \rangle}{\langle x^2 \rangle^2}, \text{ where } \langle \rangle \equiv \text{time average (1)}$$

Kurtosis is normally used to quantify deviation from Gaussian behavior. Zero mean Gaussian processes have a kurtosis of 3.0. Multiple frequency VIV response is often Gaussian in behavior, and tends to

have kurtosis values of approximately 3. The occasional occurrence of a single frequency, lock-in event is characterized by steady sinusoidal behavior. When $x(t) = \sin(\omega t)$, the kurtosis takes on the value of 1.5.

By plotting the kurtosis of a typical response measurement over time it is possible to quickly identify transitions from multi-frequency behavior to single-frequency, constant amplitude lock-in events.

Figure 1 is an example of VIV response data, taken every 48 minutes on the Scheihallion drilling riser in the North Sea. Time, spanning several days, is plotted horizontally in Figure 1. The maximum tidal current over all water depth is plotted with the kurtosis of the transverse acceleration response measured on the drilling riser at a position $z/L = 1/8$. z is the axial coordinate on the riser as measured up from the bottom, and L is the total riser length. This particular riser was in a water depth of 368 meters, and depending on the strength of the current responded with VIV in the 1st to 4th modes. The first four modes all have substantial modal amplitude at $L/8$.

Twice per day tides dominated the current and for several days in a row as shown in Figure 1, current conditions permitted one mode to dominate the vibration. At these times the response in the mode favored by the current profile built up to the point that significant VIV at different frequencies from less favorable regions of the riser was suppressed. Wake synchronization was established in the power-in region and lock-in occurred. As a result, the response grew in amplitude, was dominated by a single frequency, and the kurtosis approached 1.5, the ideal sinusoidal value. This is seen several times in Figure 1. Further discussion of the Scheihallion data is to be found in Cornut & Vandiver(2000).

This particular data covers a span of eleven days. The lowest line in the figure is the maximum current, which occurred in the entire water column, as measured by an acoustic Doppler profiler (ADCP). There is not a simple correlation between maximum current speed and lock-in events.

The prediction of a lock-in event requires examination of each current profile to determine the power-in region of each possible contending mode. One must then have a means of comparing the relative strengths of each mode. When one mode has a dominant position, then lock-in occurs and other modes are squeezed out. The next section presents a model for the prediction of single mode dominance, based on structural dynamic properties and the flow profile.

3 PREDICTING MODAL DOMINANCE

3.1 Introduction

For uniform flow lock-in problems the reduced damping parameter has long been recognized as being useful for response prediction. It has various names and forms, including the Scruton number, k_s , S_G , and ζ_s / μ . The later three are all related as follows:

$$S_G = \zeta_s / \mu = 2\pi S_t^2 k_s = 2\pi S_t^2 \frac{4\pi m \zeta_s}{\rho_w D^2}$$

$$\text{where } \zeta_s = \frac{r_s}{2\omega m}, \quad (2)$$

$m \equiv \text{mass / length}$, $\rho_w \equiv \text{mass density of water}$ and r_s is the structural damping force / length / velocity.

Vandiver(1993) showed that for uniform cylinders in uniform flow this expression simply reduces to the following:

$$S_G = \frac{r_s \omega}{\rho_w U^2} \quad (3)$$

where U is the uniform flow velocity and ω is the vibration frequency in radians/second.

This reveals that the reduced damping is simply a ratio of the damping force per unit length to the exciting force per unit length. In Vandiver(1985) a generalized reduced damping parameter is proposed for sheared flow conditions. This generalized form accounted for hydrodynamic contributions to damping and provided for separate power-in and damping zones for each potentially responding mode.

At the time the formulation was not particularly useful as a response prediction tool, because the necessary understanding of both the hydrodynamic damping and excitation was too primitive. The state of the art has advanced to the point that revisiting this approach is now fruitful. The principles are illustrated here in a series of simplified hypothetical problems.

First, consider a riser excited by a flow profile with two regions, each uniform in profile but with different speeds, as shown in Figure 2. It is assumed that the riser can be modeled as a beam under tension and can be analyzed by a modal analysis technique. To begin a few definitions from modal analysis are required.

3.2 Modal Analysis Definitions

It is assumed that some form of modal analysis may be applied. It could be done in terms of complex modes, but simpler undamped normal modes are adequate to illustrate the concepts. Complex mode analysis could be added later, with much the same result. First, the modal mass, stiffness and damping are defined, followed by modal force and modal damping ratio for mode i .

$$M_i = \int_0^L m(x) \phi_i^2(x) dx, \text{ modal mass} \quad (4)$$

$$K_i = M_i \omega_i^2, \text{ modal stiffness} \quad (5)$$

$$R_i = \int_0^L r(x) \phi_i^2(x) dx, \text{ modal damping} \quad (6)$$

$$F_i = \int_a^b f(x, t) \phi_i(x) dx, \text{ modal force} \quad (7)$$

$$\zeta_i = \frac{R_i}{2\omega_i M_i}, \text{ modal damping ratio} \quad (8)$$

where $m(x)$, $r(x)$, and $f(x, t)$ are the mass, damping and excitation per length, and ω_i is the natural frequency of mode i . With these quantities defined the dynamic response of any single mode may be written in terms of a simple, single-degree-of-freedom oscillator as shown next:

$$M_i \ddot{q}_i + R_i \dot{q}_i + K_i q_i = F_i(t), \quad (9)$$

where q_i is the modal response participation factor.

In general the response of the system is composed of the superposition of the individual modal responses, as follows:

$$w(x, t) = \sum_i q_i(t) \phi_i(x) \quad (10)$$

When $f(x, t)$ is a steady, single frequency force, the steady state response of each mode, i , may be obtained from the transfer function for mode i , as shown below.

$$\text{when, } f(x, t) = f(x) e^{i\omega t} \quad (11)$$

$$\text{then, } q_i(t) = |F_i| |H_i(\omega)| e^{i(\omega t - \psi)}, \quad (12)$$

where ψ is a phase angle and

$$|H_i(\omega)| = \frac{1/K_i}{\left[\left(1 - \frac{\omega^2}{\omega_i^2}\right)^2 + \left(2\zeta_i \frac{\omega}{\omega_i}\right)^2 \right]^{1/2}} \quad (13)$$

When the exciting frequency is at the natural frequency, the resonant response takes on the particularly simple form:

$$|q_i| = \frac{|F_i|}{K_i} \frac{1}{2\zeta_i \omega_i} = \frac{|F_i|}{R_i \omega_i} \quad (14)$$

It is of course true that other modes will also re-

spond to the same force and at the same frequency, but not resonantly. The total structural response will be composed of the summation of all of the modal responses. However, the purpose of this exercise is to determine which response frequency will dominate the response of the structure. If there is a dominant frequency in the response, then the mode which is resonant at that frequency should be a good measure of the relative response of the system at that frequency compare to other frequencies.

3.3 Lift force and hydrodynamic damping estimation in a two-flow field.

Returning to the problem shown in Figure 2. Assume that one mode dominates the response and that the power-in zone is the higher speed zone with velocity U_{hi} and that the power-out region is the region with velocity U_{low} . The magnitude of the response of the resonant mode may be computed from Equation 14. But first, expressions for the modal force and modal damping must be found.

3.3.1 Lift force in a power-in zone

The lift force per unit length is given by:

$$f(x, t) = \frac{1}{2} \rho_w DC_{L,hi} U_{hi}^2 \text{sgn}(\phi_i) \quad (15)$$

where $\text{sgn}(\phi_i)$ means sign of the undamped mode shape ϕ_i .

Assuming the mode shape has a sinusoidal form, then the modal force may be computed from Equation 7 as follows:

$$|F_i| = \int_{L_{low}}^L \phi_i(x) \text{sgn}(\phi_i(x)) f(x, t) dx \quad (16)$$

$$= \frac{1}{2} \rho DC_{L,hi} U_{hi}^2(x) \int_{L_{low}}^L \left| \sin\left(\frac{i\pi}{L} x\right) \right| dx \quad (17)$$

$$\cong L_{hi} \frac{\rho_w}{\pi} DC_{L,hi} U_{hi}^2 \quad (18)$$

where $L_{hi} = L - L_{low}$

The above final result is approximate because the integral in equation 17 has been approximated by $\frac{2}{\pi} L_{hi}$, the average value of the magnitude of the sine function multiplied by the length of the power-in region.

3.3.2 Hydrodynamic damping estimation

A formulation for hydrodynamic damping, appropriate to cross-flow vibration, is required. A suitable model is to be found in Venugopal(1996). His formulation was based on a survey of all damping data

available in the public domain literature. An improved version of his damping model is implemented in the MIT, VIV response prediction program SHEAR7, versions 2.2 & 3.0 (Vandiver & Lee, 1999). That formulation is described here. Recent experimental work by Kyrre Vikestad at Marintek has provided an independent confirmation of the validity of this damping model, (Vikestad, Larsen, & Vandiver, 2000).

The hydrodynamic damping for cross-flow VIV has two forms, one appropriate for regions with reduced velocities above that found in the power-in zone for any specific frequency, and another form appropriate for regions with reduced velocity lower than that in the power-in region.

3.3.2.1 Low- V_R model

$$r_{low}(x) = r_{sw} + C_{rl} \rho_w D U(x) \quad (19)$$

Where $C_{rl} = 0.18$ is an empirical constant and

$$r_{sw} = \frac{\omega_i \rho_w \pi D^2}{2} \left[\frac{2\sqrt{2}}{\sqrt{R_{e,\omega}}} + 0.2 \left(\frac{A}{D} \right)^2 \right] \quad (20)$$

$$\text{Where, } R_{e,\omega} = \frac{\omega_i D^2}{\nu} \quad (21)$$

is a vibration Reynolds number, and ν is the kinematic viscosity. ω_i is assumed to be the frequency of the excitation in the power-in region associated with U_{hi} .

3.3.2.2 High- V_R model

$$r_{hi}(x) = \frac{C_{rh} D \rho_w U(x)}{2\pi S^t} \frac{\omega_s}{\omega_j}, \text{ where } C_{rh} = 0.2 \quad (22)$$

The high- V_r damping model is not needed for the present example, but will be needed later.

3.4 Response of a single mode in a two speed flow

Returning to the problem illustrated in Figure 2, with the dominant frequency of excitation coming from a power-in region associated with the high flow velocity, the hydrodynamic damping comes from a flow region with a reduced velocity below that of the power-in zone. Therefore, the modal damping is of the low- V_R type given above. The excitation is at ω_i and is due to VIV associated with U_{hi} .

Solving for the modal damping

$$R_i = R_{i,s} + \int_0^{L_{low}} r_{low}(x) \phi_i^2(x) dx \quad (23)$$

$$= R_{i,s} + r_{low} \int_0^{L_{low}} \sin^2 \left(\frac{i\pi x}{L} \right) dx \quad (24)$$

$$\cong R_{i,s} + r_{low} \frac{L_{low}}{2} \quad (25)$$

where $R_{i,s}$ is the structural damping contribution, which is usually small compared to hydrodynamic sources in sheared flow. The integral has again been approximated by the average of the integrand times the range, L_{low} .

In a later example, damping of the high- V_R type will be needed. It will occur in the high speed region. Doing a similar integral as above yields for high- V_R modal damping for a mode 'j', the value:

$$R_j \cong R_{j,s} + r_{hi} \frac{L_{hi}}{2} \quad (26)$$

It is now a simple matter to use Equation (14) to find an estimate of the resonant response magnitude for mode 'i'.

$$|q_i| = \frac{|F_i|}{R_i \omega_i} = \frac{2\rho_w D C_{L,hi} U_{hi}^2 L_{hi}}{\pi \omega_i (2R_{i,s} + r_{low} L_{low})} \quad (27)$$

This equation provides considerable insight about VIV response. First consider the case that the power-in region grows to include the entire length.

3.4.1 Full length lock-in, $L_{hi} = L$

In this case $L_{low} = 0$ and Equation 27 simplifies to the following form.

$$\frac{|q_i|}{D} = \frac{\rho_w C_{L,hi} L U_{hi}^2}{\pi \omega_i R_{i,s}} \quad (28)$$

If the structural modal damping is assumed to be distributed equally along the length as a damping constant r_s , then

$$R_{i,s} = \frac{r_s L}{2} \quad (29)$$

and the above expression for response simplifies to

$$\frac{|q_i|}{D} = \frac{2C_{L,hi}}{\pi} \frac{\rho_w U_{hi}^2}{r_s \omega_i} = \frac{2C_{L,hi}}{\pi} \frac{1}{S_G} \quad (30)$$

where S_G is that shown in Equation 3. This makes clear the reason that S_G has had a strong empirical connection to response. Next consider what happens when two modes compete.

3.5 Two competing modes in a two speed flow

Again using Figure 2 as the starting point, assume the two regions of constant flow speed are each power-in regions for different modes 'i' and 'j'. The response due to the high velocity region has been found in the previous example.

The purpose of this exercise is to see which mode is likely to dominate the response. Taking the ratio of modal response amplitudes yields:

$$\left| \frac{q_i}{q_j} \right| = \left| \frac{q_{hi}}{q_{low}} \right| = \left| \frac{F_i}{F_j} \frac{R_j}{R_i} \frac{\omega_j}{\omega_i} \right| \quad (31)$$

$$\left| \frac{q_i}{q_j} \right| = \left| \frac{q_{hi}}{q_{low}} \right| = \frac{L_{hi}}{L_{low}} \frac{C_{L,hi}}{C_{L,low}} \frac{U_{hi}^2}{U_{low}^2} \frac{\omega_j}{\omega_i} \left[\frac{\frac{r_s L}{2} + r_{hi} \frac{L_{hi}}{2}}{\frac{r_s L}{2} + r_{low} \frac{L_{low}}{2}} \right] \quad (32)$$

The structural damping is usually very small compared to the hydrodynamic and can often be neglected leading to:

$$\left| \frac{q_i}{q_j} \right| = \left| \frac{q_{hi}}{q_{low}} \right| = \frac{L_{hi}}{L_{low}} \frac{C_{L,hi}}{C_{L,low}} \frac{U_{hi}^2}{U_{low}^2} \frac{\omega_j}{\omega_i} \left[\frac{r_{hi} L_{hi}}{r_{low} L_{low}} \right] \quad (33)$$

Noting that $\frac{\omega_j}{\omega_i} = \frac{U_j}{U_i} = \frac{U_{low}}{U_{hi}}$, this expression reduces to

$$\left| \frac{q_i}{q_j} \right| = \left| \frac{q_{hi}}{q_{low}} \right| = \frac{L_{hi}^2}{L_{low}^2} \frac{C_{L,hi}}{C_{L,low}} \frac{U_{hi}}{U_{low}} \frac{r_{hi}}{r_{low}} \quad (34)$$

To proceed further requires evaluation of the ratio of r_{hi} to r_{low} . The ratio of equations 22 to 19 leads to

$$\frac{r_{hi}}{r_{low}} = \frac{C_{rh} D \rho_w U_{hi}}{2\pi S_t} \frac{\omega_i}{\omega_j} \left[\frac{1}{r_{sw} + C_{rl} \rho_w D U_{low}} \right] \quad (35)$$

Where ω_i / ω_j is from the ratio ω_s / ω_j in equation 22.

In this example mode 'j' gets its power from the low velocity region at the frequency ω_j and its damping from the high velocity zone, where the local vortex shedding frequency is at $\omega_s = \omega_i$.

In many circumstances, the still water component is small compared to the rest of the low- V_r damping term and may be neglected. In this case, the previous equation reduces to

$$\frac{r_{hi}}{r_{low}} = \frac{1}{2\pi S_t} \frac{C_{rh}}{C_{rl}} \frac{U_{hi}^2}{U_{low}^2} \quad (36)$$

This yields a very useful expression for the ratio of the modal responses:

$$\left| \frac{q_i}{q_j} \right| = \left| \frac{q_{hi}}{q_{low}} \right| = \frac{1}{2\pi S_t} \frac{L_{hi}^2}{L_{low}^2} \frac{U_{hi}^3}{U_{low}^3} \frac{C_{rh}}{C_{rl}} \frac{C_{L,hi}}{C_{L,low}} \quad (37)$$

q_i is the mode participation factor for the mode excited in the high velocity region. Even though the lift coefficients for the two competing modes are unknown functions of V_R and A/D , this equation gives considerable insight as to which of two competing modes will dominate in a sheared flow. The mode driven by the higher velocity flow is favored by the ratio of the flow velocities cubed. The mode with the greater power-in length is favored by the length ratio squared. The dimensionless, empirically determined constants C_{rl} and C_{rh} are 0.18 and 0.2 respectively and approximately cancel.

The lift coefficients in the above expression will be determined by the outcome of the competition of the two modes. For the purpose of predicting the dominant mode, one might assume they are equal. Thus the ratio of the velocities and the power-in lengths are the principal parameters controlling which mode, if either will win out.

In a linear sheared flow, the mode with the higher natural frequency would tend to have the longer power-in region for the following reason. Assume two modes are in competition. If either dominates the response, it will establish lock-in over a section of the riser. There is considerable experimental evidence to suggest that the lock-in bandwidth in a sheared flow allows a variation of speed above and below the ideal lock-in speed of approximately 15 to 20%. In a linear sheared flow, ± 15 to 20% of the local velocity spans a greater portion of the length if the local velocity is high than when it is low. One might conclude that the mode in the higher flow will always win out. However, real flows are in general not linear, and the actual profile will have to be taken into consideration.

3.6 Uniform flow on a riser with two diameters

As a final instructive example, consider a uniform flow speed U . The flexible riser has two sections, one with a large diameter, D_L , such as a section with buoyancy modules, and a small diameter region with diameter, D_s . The length of each region is L_L and L_s corresponding to the large and small diameters. Vibration in response to lift forces on the large diameter is subjected to high- V_R damping in the small diameter region. Vibration driven by lift forces on the small diameter region is subjected to damping of the low- V_R type in the large diameter region.

Equations 15-18 with the appropriate diameters inserted can be used to find the modal forces for each diameter. Equations 19 and 22 give the correct high and low- V_R damping expressions when used with the correct diameters. Assuming a different mode is resonantly excited in each diameter region, Equations 14, 25 and 26 can be used to compute the resonant response of each mode.

If, as in the previous example, the structural and still water damping are assumed small and neglected, the following expression is found for the ratio of the two modal responses:

$$\frac{q_L}{q_S} = \frac{L_L^2 D_L^2 C_{rl} C_{L,L}}{L_S^2 D_S^2 C_{rh} C_{L,S}} \quad (38)$$

This shows that when a riser has two different diameters the larger diameter region is highly favored to dominate the response. The practical result of this is that the buoyant regions on a riser are most likely to control the VIV response. This was the case on the Helland Hansen riser discussed later in this paper.

3.7 Response prediction programs

In a response prediction program, such as SHEAR7, the response of each mode may be computed with no approximations made in the modal force and modal damping integrals. In addition no terms need to be ignored in the damping expressions. The program may include an algorithm, which decides when one mode will dominate and all others will be suppressed by the vibration at the dominant frequency.

This paper began by showing the measured response from a real drilling riser. When the kurtosis drops towards 1.5, this is an indication that one frequency is dominating the response and pushing out participation at other possible vortex shedding frequencies. The next section gives two actual examples, one is dominated by a single frequency and one has two frequencies present in the response.

4 RESPONSE PREDICTION

Two examples are given here to illustrate how real risers respond in real current profiles. As a part of the Norwegian Deepwater Project data was acquired on the Helland-Hansen drilling riser in 1998. It was in 684 m of water in the Norwegian North Sea. Six instrument packages recorded acceleration. The riser was mostly covered by 1.13 m diameter buoyancy, except for the top 100 meters and a few short gaps elsewhere on the riser.

Figure 3 is a plot of kurtosis, maximum current and RMS acceleration response at $z/L=0.094$ from the bottom of the riser for a span of several days in June of 1998. Two examples, A and B, have been selected at 1600 and 2000 hours. At 1600 the computed kurtosis, which used a 34 minute acceleration record, dropped to 1.6, indicating nearly ideal sinusoidal behavior. Four hours later the kurtosis rose to 2.1. Figures 4 and 5 show the corresponding current profiles, annotated with the estimated locations of the potential power-in zones.

Mode participation analysis of the response records by Froydis Solaas and Karl Erik Kaasen of Marintek revealed that in Case A the response spectra at all six measurement locations had a single dominant peak at 0.0749 Hz, the natural frequency of the third mode.

Many different combinations of critical reduced velocity and reduced velocity bandwidth were tried in order to find a combination that would predict the correct dominant mode. For the two examples shown here a value of $V_{R,crit}=3.0(S_t=0.33)$ worked the best when combined with a reduced velocity bandwidth of $\pm 20\%$ ($\frac{\Delta V_R}{V_R} = 0.4$). Using these val-

ues, Figure 4 shows the possible power-in zones for modes 1-4. The power-in zone for mode 3 is the largest predicted. Mode three did in fact dominate the response at the exclusion of the other modes. The RMS modal amplitude was 0.3 diameters.

Four hours later, Case B, the potential power-in regions for modes 1, 2 and 3 were as predicted in Figure 5, which also shows the velocity profile. Response analysis revealed two peaks at 0.0519 and 0.0734 Hz, the natural frequencies of modes 2 and 3. In this case neither mode was sufficiently dominant to suppress the VIV at the other frequency. Two frequencies appeared in the response spectra and the kurtosis was 2.1. The RMS response was approximately 0.28 diameters.

SHEAR7 Version 3.0 has built into it all of the computations described in this paper, as well as an

experimentally determined lift coefficient table which is dependent on A/D . For these two cases the SHEAR7 prediction is given in Figures 6 and 7, using the values of reduced velocity bandwidth and Strouhal numbers cited above. SHEAR7 conservatively overpredicts the response by a small amount. However, it was necessary to match the measured and predicted natural frequencies, as well as the choice of Strouhal number and reduced velocity bandwidth. Natural frequency matching was done by setting the added mass coefficient so as to correctly predict the measured third mode natural frequency in each case, A and B.

On real drilling risers the observed natural frequencies have very large variation for low modes due to large variations in added mass with reduced velocity. There is also emerging evidence that Strouhal numbers are quite sensitive to Reynolds number in the range from 100,000 to 1,000,000, as has been observed in laboratory experiments on non-moving cylinders. The exact dependence for real drilling risers is not yet known because it is a function of response A/D , roughness and turbulence. This type of proprietary data is not yet available from laboratory tests and it is very difficult to extract from full-scale measurements. Work is continuing to resolve these unknowns.

5 CONCLUSIONS

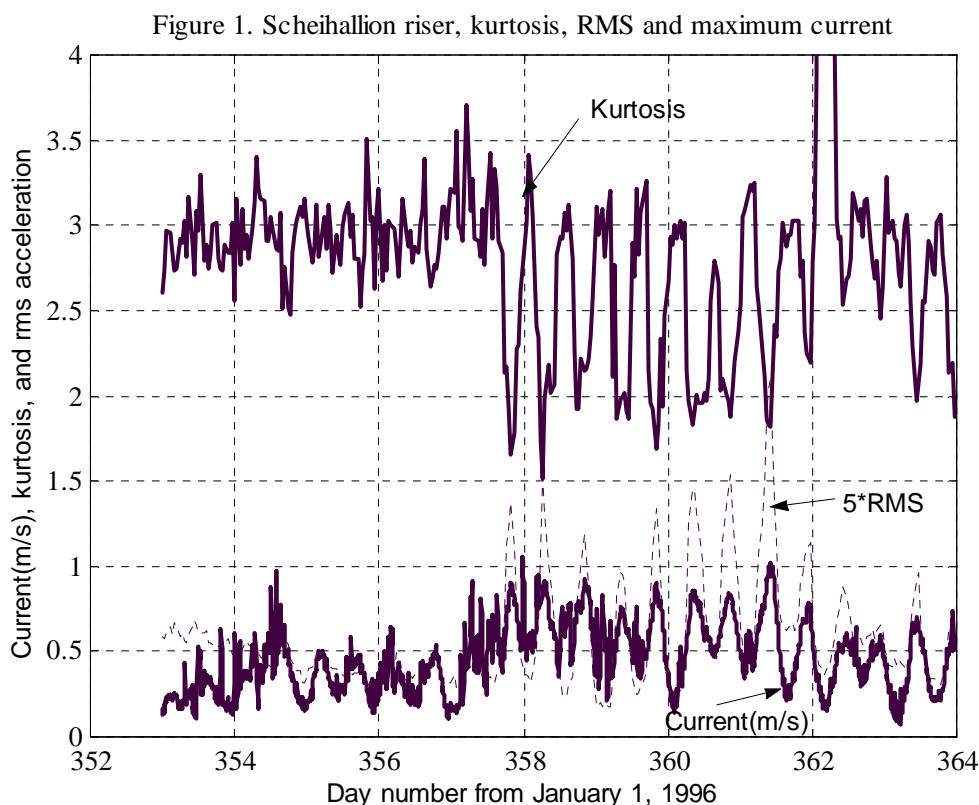
It has been shown that single frequency lock-in events may be detected in dynamic response data by means of the kurtosis statistic. An analysis is pre-

sented which reveals that single frequency dominance is most likely to be associated with the highest velocities in the profile. When a riser has variation in diameter, such as when covered with partial buoyancy, the larger diameter section is more likely to dominate the response in a uniform current. Prediction of lock-in events is difficult. The Strouhal number, reduced velocity bandwidth and natural frequencies must be correct. Natural frequency prediction is difficult, because the added mass coefficient for each mode depends on the reduced velocity distribution.

In two example cases taken from the Helland Hansen drilling riser, the Strouhal number which gave correct prediction of the dominant mode was 0.33. This value is the result of Reynolds numbers above 100,000. (261,000 at 0.3 m/s).

REFERENCES

- Cornut, S., & Vandiver, J.K., 2000, Paper No. 005022, 'Offshore VIV Monitoring at Scheihallion-Analysis of Riser VIV Response', Proc. of ETCE/OMAE2000 Joint Conference, New Orleans, February 14-17, 2000.
- Vandiver, J. K., 1985, "Prediction of Lockin Vibration on Flexible Cylinders in Sheared Flow," Proceedings of the 1985 Offshore Technology Conference, Paper No. 5006, Houston, May 1985.
- Vandiver, J.K., 1993, "Dimensionless Parameters Important to the Prediction of Vortex-Induced Vibration of Long, Flexible Cylinders in Ocean Currents", *Journal of Fluids and Structures*, Vol. 7, No. 5, pp. 423-455, July 1993.
- Vandiver, J. K., Lee, L., 1999, 'SHEAR7 Program Theoretical Manual', MIT Department of Ocean Engineering, Cambridge, MA., USA, Revised October 1999.
- Vikestad, K., Larsen, C.M., & Vandiver, J.K., 2000, 'Norwe-



gian Deepwater Riser and Mooring: Damping of Vortex-Induced Vibrations', Proc. Offshore Technology Conference 2000, Paper No. 11998., Houston, May 1-4, 2000.

Venugopal, M., 1996, 'Damping and Response Prediction of a Flexible Cylinder in a Current', Doctoral dissertation, Massachusetts Institute of Technology, Department of Ocean Engineering, Supervisor: Prof. J. K. Vandiver, Feb. 1996.

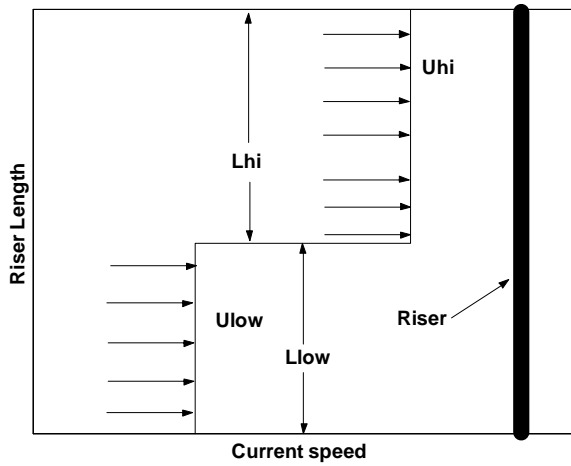


Figure 2. Two slab flows competing for VIV dominance.

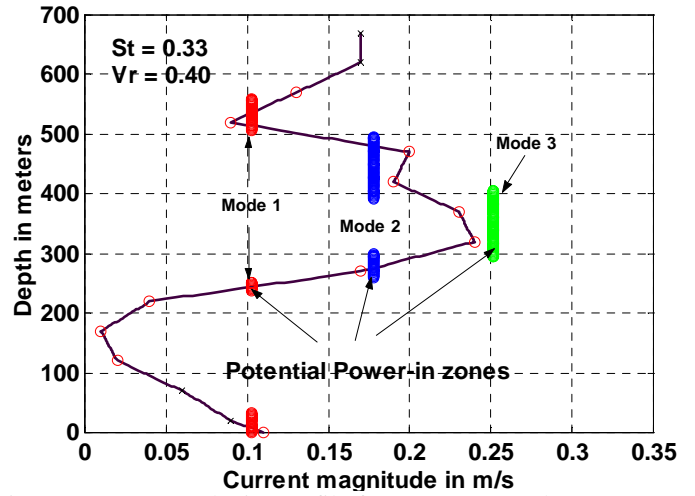


Figure 5. Case B velocity profile for, June 5, 2000 hours

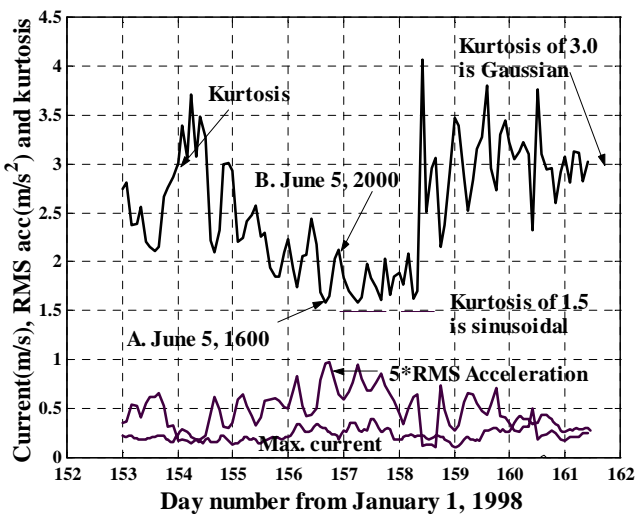


Figure 3. Helland Hansen kurtosis, RMS response and maximum current June 2-10, 1998

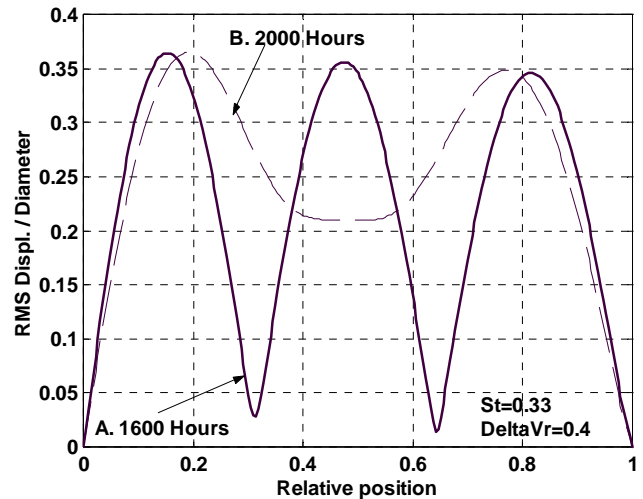


Figure 6. SHEAR7 A/D prediction for 1600 and 2000 hours on June 5, 1998.

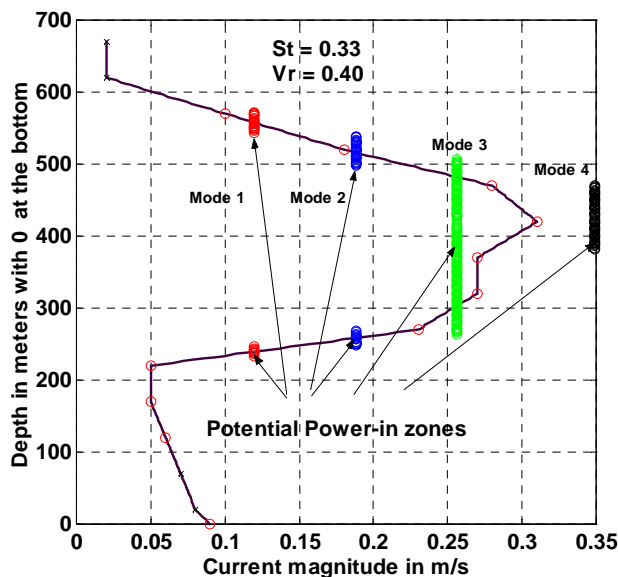


Figure 4. Case A. Third mode lock-in, 1600 hours, June 5, 1998

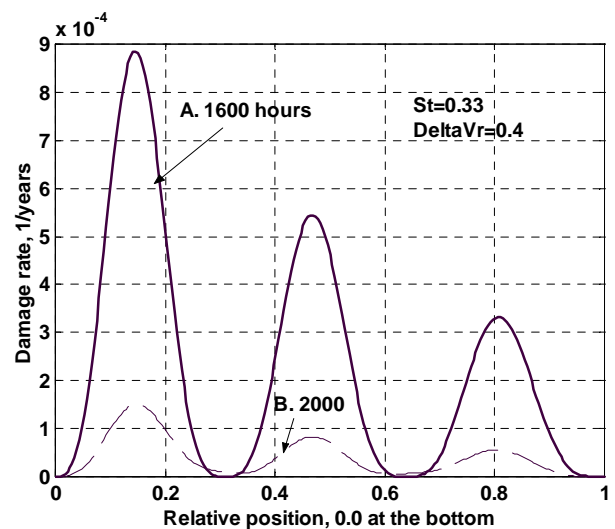


Figure 7. SHEAR7 fatigue damage rate prediction for 1600 and 2000 hours on June 5, 1998.